QCD Evolution Workshop 2013
International Journal of Modern Physics: Conference Series
Vol. 25 (2014) 1460044 (10 pages)

DOI: 10.1142/S2010194514600441

World Scientific
www.worldscientific.com

FRAGMENTATION FUNCTIONS AT BABAR*

ISABELLA GARZIA
on behalf of the BaBar Collaboration
INFN-Sezione di Ferrara and University of Ferrara, Ferrara, Italy
garzia@fe.infn.it

Published 2 January 2014

Inclusive hadron production cross section in e^+e^- annihilation shed light on fundamental questions of hadronization and fragmentation processes. We present measurements of inclusive spectra of charged pions, kaons, and protons (antiprotons) produced in e^+e^- collisions at the center-of-mass energy of 10.54 GeV, and tests of QCD predictions and hadronization models. We also report the results on the measurement of the azimuthal modulation induced by the Collins effect in inclusive production of charged pion pairs $e^+e^- \to \pi\pi X$, where the two pions are produced in opposite hemispheres. These data allows the determination of the polarized Collins fragmentation functions.

Keywords: Fragmentation functions; hadrons production.

PACS numbers: 13.66.Bc, 13.87.Fh, 12.38.Qc, 13.88.+e, 14.65.−q

1. Introduction

Fragmentation functions describe the probability for a parton (quarks or gluons) to fragment into a hadron carrying a certain fraction of the parton's energy. Fragmentation functions incorporate long distance, non-perturbative physics of the hadronization process, and cannot be calculated in perturbative QCD but can be parameterized at some fixed center-of-mass (c.m.) energy and then predicted at other energies. The cleanest environment to measure fragmentation functions is in e^+e^- annihilation experiment, since no hadrons are present in the initial state.

The process $e^+e^- \to q\bar{q} \to$hadrons can be described through three stages, as illustrated in Fig. 1. First, the quark (q) and antiquark ($\bar{q}$) fragment via radiation of gluons, each of which can radiate further gluons or split into a $q\bar{q}$ pair. This first step is calculable in perturbative QCD, but the difficulty of such calculations has limited them to low orders in α_s [1, 2] or leading logs.[3] In the following stage the produced

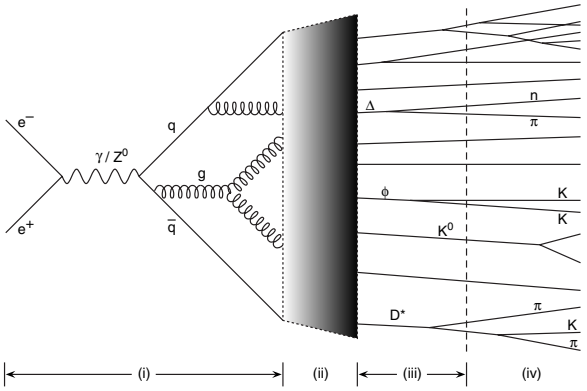

Fig. 1. Schematic picture of the $e^+e^- \to q\bar{q} \to$hadron process, as described in the text.

partons "hadronize", or transform into primary hadrons, which then decay into stable hadrons in the last stage. There are several phenomenological models used to reproduce the parton production stage and hadronization, such as JETSET,[4] HERWIG[5] and UCLA.[6] Each model contains a set of parameters used to describe the hadronization process, whose values have been tuned to reproduce data from e^+e^- annihilation experiments. One fundamental test is the study of the scaling properties, which needs accurate inclusive measurement of hadron production also at low c.m. energies (E_{CM}). Measurements performed by ARGUS[7] at the $E_{CM} \sim 10$ GeV, previous than B factories, were not able to cover the full kinematic range.

The description of the hadronization process reported above accounts only for unpolarized fragmentation. Transverse spin effects in fragmentation processes were first discussed by Collins in Ref. [8], who introduced the chiral-odd polarized fragmentation function $H_1^\perp$, also called Collins function, which describes the distribution of the final state hadrons around the momentum direction of the fragmenting quark. Direct evidence of Collins function can be obtained from e^+e^- annihilation experiments by studying the process of semi-inclusive pions production $e^+e^- \to q\bar{q} \to \pi\pi X$, where the two charged pions, coming from the fragmentation of a q and a $\bar{q}$ ($q = u, d, s$) with opposite transverse spin component, are detected simultaneously. In e^+e^- annihilation, the measurement of the Collins effect can be performed in two different reference frames,[9] described in Fig. 2. We refer to them as the thrust reference frame or RF12 (Fig. 2(left)), and the second hadron reference frame or RF0 (Fig. 2(right)). The normalized cross section in the e^+e^- c.m. system is proportional to

$$\sigma \propto 1 + \sin^2(\theta)\cos(\phi)\frac{H_1^\perp(z_1, \mathbf{p}_{\perp 1})\overline{H}_1^\perp(z_2, \mathbf{p}_{\perp 2})}{D_1^\perp(z_1, \mathbf{p}_{\perp 1})\overline{D}_1^\perp(z_2, \mathbf{p}_{\perp 2})}, \tag{1}$$

where D_1 is the well known unpolarized fragmentation function, the bar denotes the $\bar{q}$ fragmentation, $z = 2E_\pi/E_{CM}$ is the pion fractional energy, $\mathbf{p}_\perp$ is the transverse

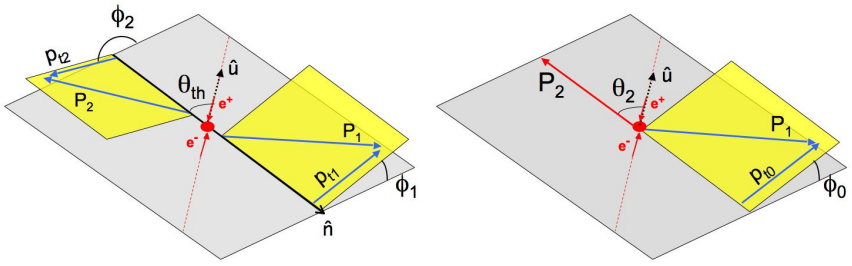

Fig. 2. (a) Thrust reference frame or RF12: $\theta = \theta_{th}$ is the angle between the e^+e^- collision axis and the thrust axis ($\hat{n}$),[11] $\phi_{1,2}$ are the azimuthal angles between the scattering plane and the momentum transverse to the thrust axis, $\mathbf{p}_{t1,t2}$. Note that the thrust axis provides a good approximation to the $q\bar{q}$ axis, so that $\mathbf{p}_{ti} \simeq \mathbf{p}_{\perp i}$ in Eq. (1). (b) Second hadron frame or RF0: θ_2 is the angle between the beam axis and the second hadron momentum P_2; ϕ_0 is the azimuthal angle between the plane defined by the beam axis and P_2, and the first hadron's transverse momentum $\mathbf{p}_{t0}$. All tracks are boosted to the e^+e^- center of mass frame.

momentum of the pion with respect to the $q\bar{q}$ direction, θ is the polar angle of the analysis axis with respect to the beam axis, and ϕ is a proper combination of the pion azimuthal angles ($\phi_1 + \phi_2$ in RF12, or $2\phi_0$ in RF0 as defined in Fig. 2). The $\cos\phi$ term in Eq. (1) produces an azimuthal modulation around the $q\bar{q}$ axis, called Collins effect or Collins asymmetry. The first measurement of the Collins effect in e^+e^- annihilation experiments was performed by the Belle Collaboration,[16] which studied in detail the dependence of the asymmetry as a function of the pion fractional energies z and polar angles θ.

In the first part of this report we present measurements of cross sections for inclusive production of charged pions, kaons, and protons (antiprotons) at the c.m. energy $\sqrt{s} = 10.54$ GeV, using a relatively small sample of data from the BaBar experiment at the PEP-II B factory at the SLAC National Accelerator Laboratory. In the second part, we report the results on the measurement of azimuthal modulations (Collins asymmetries) using approximatively the full BaBar data sample. In particular, we check the Belle's results, and we study also the behavior of the asymmetry as a function of the transverse momentum p_t of pions with respect to the analysis axis.

2. Measurements of the Differential Cross Section for Inclusive Production of $\pi^\pm$, $K^\pm$, and $p/\bar{p}$.

The data used in this analysis[12] correspond to an integrated luminosity of 0.91 fb^{-1} at a c.m. energy of 10.54 GeV. In parallel, 3.6 fb^{-1} of data recorded at the $\Upsilon(4S)$ resonance ($E_{CM} = 10.58$ GeV) are also analyzed. The latter sample provides independent, stringent systematic checks, and the combined samples provide data-driven calibrations of the tracking and particle identification performance.

We select good reconstructed charged tracks from multi-hadronic events, coming from the primary interaction point, in order to minimize backgrounds from other physics process. The identification of charged tracks as pions, kaons or protons is performed using an algorithm that combines the momentum and ionization energy loss (dE/dx) measured in the Drift Chamber[13] (DCH) and the velocity measured via the Cherenkov angle in the DIRC detector.[13] The dE/dx measurements from the DCH provide good separation between low momentum particles, i.e. between $K^{\pm}$ and $\pi^{\pm}$ ($p/\bar{p}$ and $K^{\pm}$) below 0.5 (0.8) GeV/c, while the Cherenkov angle measurement from the DIRC provides a very good separation between particles with momentum from the Cherenkov threshold to about 4 GeV/c for $\pi^{\pm}$ vs. $K^{\pm}$ and 6.5 GeV/c for $K^{\pm}$ vs. $p/\bar{p}$. The performance of the hadron identification algorithm is described in terms of a momentum-dependent efficiency matrix **E**, where each element E_{ij} represents the probability that a selected track from the true i-hadron is identified as a j-hadron, with i, $j = \pi$, K p. We calibrate the efficiency matrix using samples of tracks with known hadron content and characteristics as similar as possible to our selected tracks, and we derive corrections to the simulated E_{ij} that vary smoothly with momentum and polar angle in the laboratory frame. We extract the raw differential cross section per selected events per unit momentum p_{lab} in the laboratory frame ($(1/N_{evts})dn_{\pi,K,p}/dp_{lab}$) from our sample of identified pions, kaons and protons using the corrected efficiency matrix. Then we subtract backgrounds and correct the spectra for the effects of detector efficiency and resolution, and the event selection procedure. Finally, we transform the cross sections into the e^+e^- CM frame in order to obtain the corrected differential cross sections $(1/N_{evts})dn_{\pi,K,p}/dp$. All possible systematic effects are carefully studied: the main contributions come from particle identification, tracking efficiency, and background estimate. The statistical uncertainties are much smaller than the systematic uncertainties, with few exceptions at the highest momentum, and lower momentum for proton.

Figure 3 shows the differential cross sections for π, K, and $p/\bar{p}$ as a function of scaled momentum $x_p = 2p_{CM}/E_{CM}$ (black points), and the comparison with the predictions of JETSET, UCLA and HERWIG models. Both statistical and systematic errors are included. Note that our results are very precise and extend up to $x_p \simeq 1$, and that all the three models does not describe any spectrum in detail.

2.1. *Scaling properties*

In Fig. 4, we compare our results with those obtained at higher energies from TASSO at 34 GeV[14] and SLD at 91.2 GeV.[15] The nearly full kinematic range coverage and the high precision of BaBar and SLD data, allow to study scaling properties of hadronization and to test predictions of different models of hadronization. Since QCD should be scale invariant, scaling violation effects are expected at low x_p due to the mass of hadrons, while at higher momentum substantial scaling violation is expected because of the running of the strong coupling α_s.

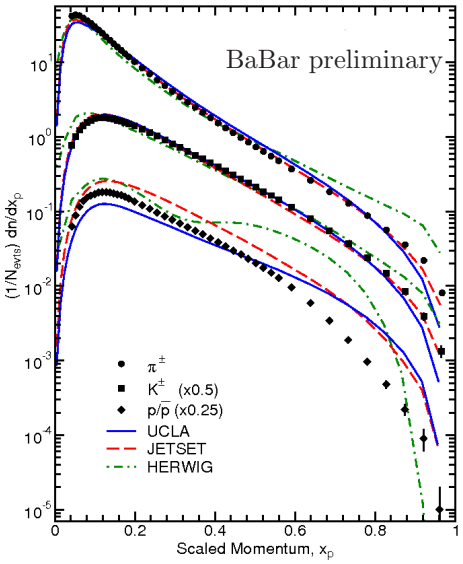

Fig. 3. Measured differential cross sections for $\pi^\pm$ (top), $K^\pm$ (middle) and $p/\bar{p}$ (bottom) in $e^+e^- \to q\bar{q}$ events. The predictions of JETSET (dashed line), UCLA (solid) and HERWIG (dotted) hadronization models are also shown.

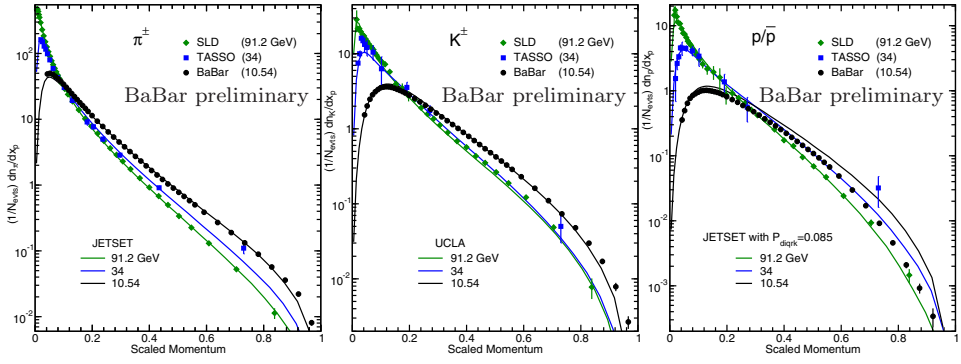

Fig. 4. Differential cross sections for pions (left), kaons (middle), and proton (right) measured at three different c.m. energies: 10.54 GeV (BABAR, black points), 34 GeV (TASSO, blue squares), and 91.2 GeV (SLD, green diamonds). Predictions by JETSET (for pions and protons) and UCLA (for kaons) are superimposed to the data point following the same color code.

This behavior for pions is well reproduced by most of the hadronization models, and in Fig. 4(left) the JETSET prediction is shown. It provides a good description of all the three data sets using the default parameters[a], and describes the high-x_p

[a]The default parameters have been chosen based on previous data, mostly at the peak of the Z^0 boson, but including the ARGUS data.

scaling violation well. The middle plot in Fig. 4 shows the cross sections for $K^{\pm}$. In this case, the different flavor composition of the three samples modifies the expected scaling, and a difference of about 15% between models and data is observed. Finally, for $p/\bar{p}$ (Fig. 4(right)), the prediction for 10.54 GeV is consistent with BaBar results for $x_p < 0.07$, but it exceeds data point for higher x_p. In particular, no model predicts the correct scaling violation for protons, even though they describe well the properties for pions. These results will be used as inputs for tuning the simulation of fragmentation processes down to an energy of 10 GeV.

2.2. *Test of QCD predictions in the MLLA model*

These data can also be used to test some predictions of QCD in the Modified Leading Logarithm Approximation (MLLA),[3] combined with the ansatz of Local Parton-Hadron Duality (LPHD).[3] For this purpose, it is convenient to plot the cross sections as a function of the variable $\xi = -\ln(x_p)$. MLLA predicts that a Gaussian function should provide a good description of these spectra around the peak position ξ^*, and that a slightly distorted Gaussian function should fit the data points over a wider range. Furthermore, the peak position ξ^*, should decrease exponentially with increasing hadron mass at a given E_{CM}.

Figure 5 shows the distributions for $\pi^{\pm}$, $K^{\pm}$, and $p/\bar{p}$ with the results of the fits. The distorted Gaussian is able to describe the BaBar data at the few percent level over a large range of ξ. In addition, we find that ξ^*_{π} is higher than ξ^*_K, in agreement with the predicted drop with hadron mass, but the ξ^*_p is not lower than ξ^*_K and thus inconsistent with the expected exponential decrease. This qualitative behavior is also observed at higher energies, where baryons and mesons appear to follow different trajectories, but measurements for more particles at $E_{CM} \sim 10$ GeV would be needed to draw any definite conclusion.

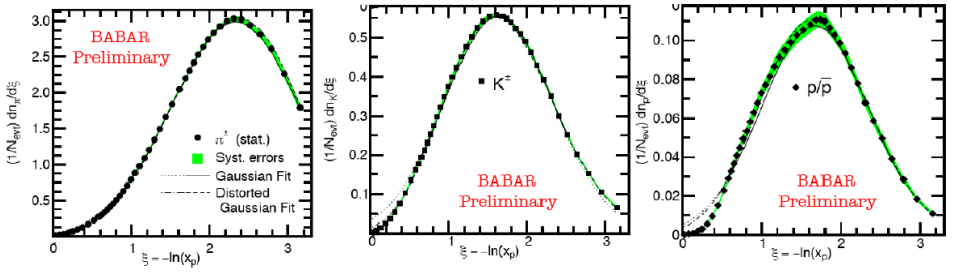

Fig. 5. Differential cross sections vs. ξ variable for pions (left), kaons (middle), and $p/\bar{p}$(right). The error bar are statistical only, while the grey bands represent the systematic uncertainties. There are also shown the results of the Gaussian (solid line) and distorted Gaussian (dashed lines) fits.

3. Measurement of the Collins effect

3.1. *Analysis strategy*

The data used for this analysis correspond to an integrated luminosity of 468 fb^{-1} collected at the $E_{CM} \sim 10.6$ GeV. The $q\bar{q}$ axis is not accessible in e^+e^- annihilation experiments, but can be approximated well by the thrust axis, which is defined as that axis that maximize the longitudinal momentum of the particles in an event.[11] We select charged pions in opposite hemispheres with respect to the thrust axis, and we measure the azimuthal angles ϕ_1, ϕ_2, and ϕ_0, as defined in Fig. 2. In order to select the two-jet topology, an event thrust value larger than 0.8 is required [b]. Only pions coming from the primary vertex with a fractional energy z in the range between 0.15 to 0.9 are selected. The Collins asymmetry can be accessed by measuring the $\cos\phi$ modulation of the normalized distributions of the selected pion pairs (Eq. (1)). However, the resulting asymmetry is largely affected by detector acceptance effects, making this measure unreliable. To reduce these fake azimuthal modulations, we construct suitable ratios of normalized distributions by selecting combinations of pions with same charge (L=like), opposite charge (U=unlike), and the sum of the two samples (C=charged), which are fitted with a function linear in $\cos\phi$:

$$\frac{N^U(\phi_i)/ < N^U >}{N^{L(C)}(\phi_i)/ < N^{L(C)} >} = B_{i,UL(UC)} + A_{i,UL(UC)} \cdot \cos(\phi_i). \tag{2}$$

The A_i parameter in Eq. (2) is sensitive to the Collins effect, $i = 12$ or $i = 0$ identifies the reference frame (RF12 or RF0), $\phi_i = \phi_1 + \phi_2$ or $\phi_i = 2\phi_0$, $N(\phi_i)$ is the di-pion yield, and $< N >$ is the average bin content. The ratios thus constructed allow to be sensitive to the favored and disfavored fragmentation functions. For example, considering the production of U pion pair ($\pi^{\pm}\pi^{\mp}$) from a $u\bar{u}$ pair, the following fragmentation processes can accour: $u \to \pi^+$ and $\bar{u} \to \pi^-$, or $u \to \pi^-$ and $\bar{u} \to \pi^+$. The first two are described by a favored fragmentation function, since the u ($\bar{u}$) is a valence quark of the π^+ (π^-), while $u \to \pi^-$ ($\bar{u} \to \pi^+$) is described by a disfavored function. Following the same procedure for L and C pion pairs, we can easily verify that the ratios in Eq. 2 contain different combination of favored and disfavored fragmentation functions.[18]

Thanks to the large amount of data we are able to choose a 6×6 (z_1, z_2) matrix of intervals, with boundaries $z_i = 0.15$, 0.2, 0.3, 0.4, 0.5, 0.7, 0.9, and the following p_t intervals: $p_t < 0.25$ GeV/c, $0.25 < p_t < 0.5$ GeV/c, $0.5 < p_t < 0.75$ GeV/c, and $p_t > 0.75$ GeV/c.

[b]The event thrust value ranges between 0.5 to 1. The lower the thrust is, the more spherical is the event. The higher the thrust is, the more jet-like is the event.

3.2. *Study of systematic effects and background contributions*

A crucial point for the measurement of the Collins asymmetries is the identification of all the systematic effects that can influence the azimuthal distributions for pion pairs. We test the double ratio method on a Monte Carlo (MC) sample, we study the influence of the particle identification, the uncertainties due to the fit procedure, and other minor effects. Using a MC sample, we evaluate the dilution of the asymmetry due to the approximation of the thrust axis as the $q\bar{q}$ direction, and due to the tracking reconstruction efficiency. When the systematic effects are sizable we correct the measured asymmetries for them and assign appropriate systematic uncertainties. All systematic uncertainties and/or corrections are evaluated for each interval of fractional energies z and transverse momenta p_t.

Background processes, like $e^+e^- \to \tau^+\tau^-$, $e^+e^- \to c\bar{c}$, and $e^+e^- \to \Upsilon(4S) \to B\bar{B}$, can introduce azimuthal modulation not related to the Collins effect. We refer to them as τ, charm, and bottom backgrounds, respectively. The asymmetry A^{meas} measured by fitting the double ratio of Eq. (2) can include the azimuthal dependence of the above processes, and can be written as:

$$A^{meas} = (1 - \sum_i F_i) \cdot A^{uds} + \sum_i F_i \cdot A^i, \tag{3}$$

where F_i and A_i are respectively the fraction of pion pairs and the asymmetry due to the i^{th} background component, with $i = \tau$, charm, or bottom, which are determined using both MC and data samples specific to each process. The fraction F_{bottom} is very low (less than 2%), while F_τ is relevant only for very energetic tracks. In addition, the asymmetries measured in a τ-enhanced data sample is consistent with zero. For these reasons, in Eq. (3), we set $A_\tau = A_{bottom} = 0$. The charm contribution, instead, is the dominant background ($F_{charm} \sim 30\%$ on average); both fragmentation and weak decay can introduce azimuthal modulations. To estimate this contribution we select a charm-enhanced data sample requiring at least one D^* candidate from the decay $D^{*\pm} \to D^0\pi^\pm$. Given A^{meas} in the full data sample and A^{D^*} in the charm-enhanced sample, we extract the real contribution from light quarks to the Collins asymmetry (A^{uds}).

3.3. *Results*

We study the behavior of the Collins effect in the RF12 and RF0 frames as a function of pion fractional energy z, pion transverse momentum p_t, and polar angle of the analysis axis.

Figure 6 shows a comparison between BaBar and Belle results as a function of z for the U/L double ratio. For this comparison, we use eleven symmetric z-bin subdivisions under $z_1 \leftrightarrow z_2$ exchange with the following boundaries: 0.15, 0.2, 0.3, 0.5, 0.7, 0.9, and we take the average of the results which fall in the same symmetrized bin. Note that in the Belle analysis z ranges between 0.2 to 1, so no result is present in the first bin, while the last bin extends up to 1. We observe

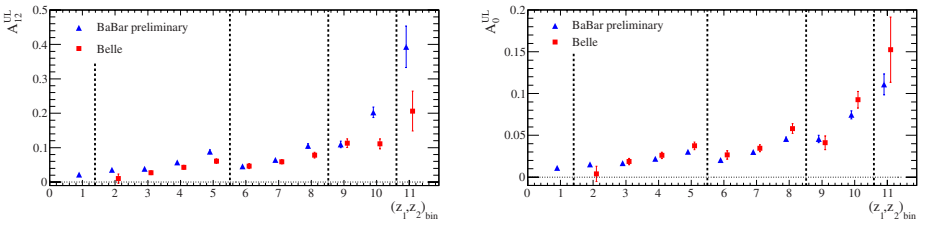

Fig. 6. Comparison between BaBar (triangles) and Belle (squares) asymmetries as a function of z obtained from the fit of the U/L double ratio (Eq. 2) in the RF12 (left) and RF0 (right) frames. Excluding the first bin for which only BaBar result is present, each region delimited by dotted line is obtained by fixing z_1 and ranging z_2. For example, the four bins between 2 to 5 are obtained by setting $0.2 < z_1 < 0.3$ and ranging z_2 between $0.2 - 0.9$; the next three points by setting $0.3 < z_1 < 0.5$ and ranging z_2 between $0.3 - 0.9$; the next two points by setting $0.5 < z_1 < 0.7$ and ranging z_2 between $0.5 - 0.9$; and finally the last point is the bin with $0.7 < z_1$, $z_2 < 0.9$. Systematic and statistical errors are included.

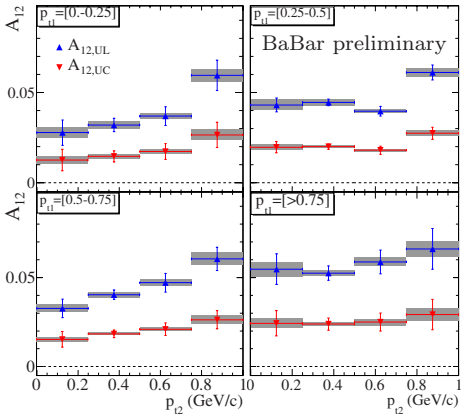

Fig. 7. Collins asymmetry for light quarks as a function of (p_{t1}, p_{t2}) intervals. Blue triangles refer to the U/L ratio, while red triangles to the U/C ratio. Statistical and systematic errors are shown as error bars and bands around the points, respectively.

a strong increase of the asymmetry as a function of z, which is in overall good agreement with Belle results in the RF0 frame. Small discrepancies are present in RF12, more evident in the last two bins where z is high. The origin of this difference is due to a different procedure on the calculation of the correction factors, which we evaluate independently for each bins of z, and to the cut on $z < 0.9$ needed to remove contamination from $e^+e^- \to \mu^+\mu^-\gamma$ events, with $\gamma \to e^+e^-$ conversion. Similar behavior is observed for the U/C double ratio.

Figure 7 shows the behavior of the Collins asymmetry in the RF12 frame as a function of p_t. No previous data from e^+e^- annihilation are available for a comparison. This dependence was studied only in the space-like region at low $|Q^2|$

(~ 2.4 (GeV/c)^2),[19] and thus can be used to investigate the evolution of the Collins function.

4. Summary and conclusions

Preliminary precision measurements of the differential cross section for charged pion, kaons and protons (antiprotons) have been performed at BaBar at $E_{CM} = 10.54$ GeV. They cover a wide range of scaled momentum x_p, and will be very valuable for a better understanding of the unpolarized fragmentation process, and to study the scaling properties down to the energy of 10 GeV. In particular, the discrepancies between data and Monte Carlo predictions on scaling violation give important experimental inputs for tuning hadronization models.

We have also reported preliminary results on the pions Collins asymmetries. In particular, we extend our analysis to the study of asymmetry behavior as a function of p_t, which may help to shed light on the evolution of the polarized Collins fragmentation functions. These data, together with the dependence of the asymmetry as a function of z, can be valuable for improving global analyses, such as performed by the authors of Ref. [20].

References

1. See e.g. R.K. Ellis, D.A. Ross and A.E. Terrano, *Nucl. Phys. B* **178**, 421 (1981).
2. See e.g. S. Moretti, *Phys. Lett. B* **420**, 367 (1998).
3. Y.I. Azimov, Y.L. Dokshitzer, V.A. Khoze and S.I. Troian, *Z. Phys. C* **27**, 65 (1985).
4. T. Sjostrand, *Comput. Phys. Commun.* **82**, 74 (1995).
5. G. Corcella *et al.*, *JHEP 0101*, 010 (2001); G. Marchesini et al., *Comput. Phys. Commun.* **67**, 465 (1992).
6. S. Chun and C. Buchanan, *Phys. Rep.* **292**, 239 (1998).
7. ARGUS Collaboration (H. Albrecht *et al.*) , *Z. Phys. C* **44**, 547 (1989).
8. J. C. Collins, *Nucl. Phys. B* **396**, 161 (1993).
9. D. Boer, *Nucl. Phys. B* **806**, 23 (2009).
10. Belle Collaboration (R. Seidl *et al.*, *Phys. Rev. Lett.* **96**, 232002 (2006).
11. E. Farhi, *Phys. Rev. Lett.* **39**, 1587 (1977).
12. BABAR Collaboration (J.P. Lees *et al.*), arXiv:1306.2895 (2013).
13. BABAR Collaboration (B. Aubert *et al.*), arXiv:1305.3560 (2013).
14. TASSO Collaboration (W. Braunschweig *et al.*) *Z. Phys. C* **42**, 189 (1989).
15. SLD Collaboration (K. Abe *at al.*), *Phys. Rev. D* **59**, 052001 (1999).
16. Belle Collaboration (R. Seidl *et al.*), *Phys. Rev. Lett.* **96**, 232002 (2006); *Phys. Rev. D* **78**, 032011 (2008); *Phys. Rev. D* **86**, 039905(E) (2012).
17. B. Aubert *et al.*, (BABAR collaboration), *Nucl. Instrum. Meth. A* **479**, 1 (2002).
18. A.V. Efremov, K. Goeke, and P. Schweitzer, *Phys. Rev. D* **73**, 094025 (2006).
19. HERMES Collaboration (A. Airapetian *et al.*) , *Phys. Rev. Lett.* **94**, 012002, (2005); COMPASS Collaboration (E. Ageev *et al.*), *Nucl. Phys. B* **765**, 31 (2007).
20. M. Anselmino *et al.*, *Phys. Rev. D* **75**, 054032 (2007).